Separation Science and Technology
Publication details, including instructions for authors and subscription information:
http://www.informaworld.com/smpp/title~content=t713708471

Numerical Study of Particle Behaviour in Split-Flow Thin-Channel Fractionation Using the Discrete Element Method

Myhuong Nguyen[a]; Martin Rhodes[a]; Kurt Liffman[b]; Ian McKinnon[c]; Ron Beckett[c]
[a] Department of Chemical Engineering, Monash University, Clayton Campus, Australia [b] CSIRO MSE, Highett, Australia [c] School of Chemistry, Monash University, Clayton Campus, Australia

Online publication date: 22 June 2010

To cite this Article Nguyen, Myhuong , Rhodes, Martin , Liffman, Kurt , McKinnon, Ian and Beckett, Ron(2008) 'Numerical Study of Particle Behaviour in Split-Flow Thin-Channel Fractionation Using the Discrete Element Method', Separation Science and Technology, 43: 11, 2981 — 3002
To link to this Article: DOI: 10.1080/01496390802221782
URL: http://dx.doi.org/10.1080/01496390802221782

Separation Science and Technology, 43: 2981–3002, 2008

ISSN: 0149-6395 print/1520-5754 online
DOI: 10.1080/01496390802221782

Taylor & Francis
Taylor & Francis Group

Numerical Study of Particle Behaviour in Split-Flow Thin-Channel Fractionation Using the Discrete Element Method

Myhuong Nguyen,[1] Martin Rhodes,[1] Kurt Liffman,[2] Ian McKinnon[3] and Ron Beckett[3]

[1]Department of Chemical Engineering, Monash University, Clayton Campus, Australia
[2]CSIRO MSE, Highett, Australia
[3]School of Chemistry, Monash University, Clayton Campus, Australia

Abstract: This study examines the usefulness of the discrete element method (DEM) for studying particle motion in SPLITT fractionation. The method was tested against the conventional SPLITT theory and published experimental data for particle sizes 7, 10, and 15 μm at various run conditions and good agreement was achieved. Illustrative studies presented in this paper show that particle collisions occur at concentrations as low as 0.05%(v/v); and particle trajectory deviates from theory more notably for larger particles, 15 μm diameter and greater. The finding suggests the DEM can be useful in SPLITT calculations for modeling the influence of particle-particle interactions.

Keywords: Numerical study, particle separation, SPLITT fractionation, the discrete element method

BACKGROUND

SPLITT or split-flow thin-channel fractionation is a continuous separation method related to the field-flow fractionation (FFF) family of analytical separation techniques, which have been widely used in many applications dealing with particulate and macromolecular samples

Received 21 December 2007; accepted 2 May 2008.
Address correspondence to Myhuong Nguyen, Department of Chemical Engineering, Monash University, Clayton Campus 3800, Australia. E-mail: myhuong.nguyen@sci.monash.edu.au

(1,2,3). First introduced in 1985 by the late J. Calvin Giddings (4), SPLITT techniques have been steadily developed for a diverse range of samples such as environmental sediment samples (5,6), blood samples (7), pharmaceutical emulsions (8), and biological cells (9).

The general separation principle of the SPLITT technique is illustrated in Fig. 1 and is briefly described below. Further information about the SPLITT technique can be obtained from the literature (4,10).

Sample suspension and carrier fluid are continuously introduced into the channel via inlets (a′) and (b′) respectively. An external force field is applied across the SPLITT channel to influence the differential, transverse transport of the particles. The field has commonly been gravitational (10,11), but can also be centrifugal (7,12), electrical (13–15), magnetic (16,17), or acoustic (18,19). A binary split of the suspended particulate samples is achieved and the two fractions are collected at the outlets (a) and (b). For gravitational SPLITT fractionation with uniform density, the fraction from outlet (a) contains particles with a smaller diameter, relative to a cut-off value, and the other fraction (outlet (b)) contains particles having a greater diameter. The cut-off value is determined by adjusting the inlet and outlet flow rates and the field strength (for further details see the Theory Section below).

Ideal SPLITT operation requires laminar flow throughout the channel. Under such a condition, parabolic profiles for the carrier flow may be used to calculate the channel fluid velocity, except in the two small regions around the inlet and outlet splitters (20,21). The Stokes number for such systems is small, therefore, particles are believed to exactly follow the fluid motion down stream (22,23). Particle-particle collisions and particle-channel wall collisions are usually assumed to be negligible in number at the low particle concentrations that are typically used ($\sim$0.1 %(v/v)).

These assumed ideal conditions have been used in a relatively simple theory to quantitatively describe the SPLITT separation processes, and

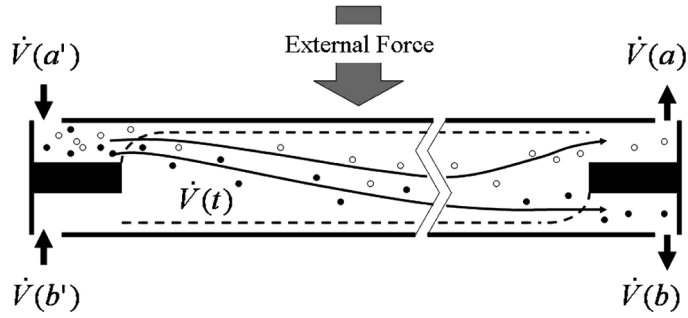

Figure 1. Illustration of the separation mechanism in a SPLITT channel.

there is reasonably satisfactory agreement between theory and experimental results (7,10). However, there are a number of undesired phenomena, believed due to some degree of fluid mixing, that have been observed (24–26). In order to improve the technique's performance, both analytical and numerical approaches have attempted to obtain insight into the particle and fluid behavior within the SPLITT micro-channel (17,21,24–26).

The availability of commercial computational fluid dynamics (CFD) software has made it potentially easier to numerically study the fluid flow behaviour in a SPLITT system. Despite being widely used in many scientific and engineering applications (27,28), the CFD approach has only recently been applied to the field of SPLITT flow. Fuh et al. (29) employed CFD to investigate fluid flow behaviour in SPLITT channels. They reported that vortex flow could be active at high inlet flows ratio and disturb the required laminar flow condition. The group then used the CFD simulation to identify a range of flow conditions in which SPLITT fractionation can be carried out without concern for hydrodynamic disturbances. They found that tapered splitter edge may be used to minimize the vortex. Thanks to this result, tapered splitters are now commonly used in SPLITT experimental set-ups. CFD has also proved useful to study edge effects on non-specific crossover due to splitter imperfections in annular SPLITT channels (30,31). The effect of several fluid forces upon particle motion, such as Basset force, drag force, and lift forces, has also been discussed in a number of SPLITT studies using the CFD method (23,32,33). In these studies, the CFD simulation approach helps to obtain two dimensional fluid flows at regions around the two splitters, where the parabolic fluid velocity profile can not be applied, therefore providing more accurate particle trajectories assuming particles being mass points. In addition, numerical modelling and simulation allows researchers to combine the effects of the particle-liquid forces in a relatively simple way.

Consistent results between simulation and experimental data from these investigations confirm the applicability of computational simulation in SPLITT studies. Additional questions to be explored are how the discrete volume of particle, or particle–particle interactions affects the overall behaviour of particles and fluid in the system? At what sample concentration or at what particle size will such effects become of concern? Among the simulation approaches available in the literature, the discrete element method (DEM) has proved to be very effective in numerous studies for particulate systems (34–39).

The DEM is a family of numerical methods for computing the motion of a large number of particles. The method was pioneered by Cundall and Strack (34) in 1979 and now has a wide range of applications

for particulate systems consisting of particles from a boulder size down to colloidal size (35–39). It would be desirable for SPLITT workers to take the advantage of this powerful approach to explore its potential use in SPLITT studies.

The use of the DEM in SPLITT studies was first mentioned by Nguyen et al. (32) Here, we further examine the usefulness of the method in SPLITT fractionation using two selected case studies, particle collision and two-way coupling of particle-fluid interactions. Similar to approaches reported by Fuh et al. (29) and Zhang et al. (23,33), in this DEM work, two dimensional (2D) fluid is used. However, in this current approach particle discrete volume is included in our computational algorithm, so that particle collisions and the effect of particle momentum on the surrounding fluid can now be quantified. Inter-particle forces are not included into the algorithm at this stage. An in-house computer code was used to generate simulation models, and the simulation was validated using published experimental SPLITT fractionation data. The source code provides the flexibility needed for our tests, which could disable or enable the effects of particle discrete volume and/or particle-particle and particle-fluid interactions on particle trajectory. Note that when these effects are disabled, the numerical algorithm is similar to that given in Zhang et al. (23).

SPLITT THEORY

The simple theory of separation in SPLITT channels based mainly on horizontal fluid flow and vertical particle settlement (Fig. 1) has been well described in numerous SPLITT publications as listed in the Introduction. It can be summarized as follows.
From Fig 1,

$$\dot{V}(t) = \dot{V}(a) - \dot{V}(a') = \dot{V}(b') - \dot{V}(b). \tag{1}$$

If F_b is the fraction of a monodisperse population exiting with substream b, then

$$F_b = 1 \text{ for } \dot{V}(t) + \dot{V}(a') \leq \Delta\dot{V}, \tag{2}$$

and

$$F_b = 0 \text{ for } \dot{V}(t) \geq \Delta\dot{V}. \tag{3}$$

where, $\Delta\dot{V}$ is the crossed volume of fluid carrying a particle downstream, and is calculated from

$$\Delta\dot{V} = bUL. \tag{4}$$

Between these above two cases, particles exit the channel via substream (a) or (b) depending on the particle stream plane (see Springston et al. (10) for detail explanation), and F_b can be represented as

$$F_b = \frac{\Delta\dot{V} + \dot{V}(a')}{\dot{V}(a')} - \frac{\dot{V}(a)}{\dot{V}(a')}. \tag{5}$$

There exists a critical particle transverse velocity, U_c, which divides the particle population between the (a) and (b) exit substreams:

$$U_c = \frac{\dot{V}(t)}{bL}. \tag{6}$$

Particles having a transverse velocity greater than the critical value will exit substream (b).

In this study, the simplest form of SPLITT fractionation, the gravitational SPLITT was used. In this case, U is the terminal velocity of particles and is described by the formula:

$$U = \frac{\Delta\rho g d^2}{18\eta}, \tag{7}$$

From Eqs. (6) and (7), there exists a critical particle diameter, d_c, above which particles will exit (b):

$$d_c = 3\left(\frac{2\eta\dot{V}(t)}{\Delta\rho g b L}\right)^{\frac{1}{2}} \tag{8}$$

NUMERICAL METHOD

Numerical study of particle trajectories is based on the general theory of the discrete element method (DEM) for particle motion in a fluid flow.

Numerical Modeling of the Fluid Flow in a SPLITT Thin Channel

The governing equations used in fluid simulation are: the continuity:

$$\frac{\partial u}{\partial x} + \frac{\partial v}{\partial y} = 0, \tag{9}$$

and the Navier-Stokes equations for a dimensionless 2D incompressible viscous flow (40)

$$\frac{\partial u}{\partial t}+u\frac{\partial u}{\partial x}+v\frac{\partial u}{\partial y}=-\frac{\partial p}{\partial x}+\frac{1}{\mathrm{Re}}\left(\frac{\partial^2 u}{\partial x^2}+\frac{\partial^2 u}{\partial y^2}\right)+f_x, \tag{10}$$

and

$$\frac{\partial v}{\partial t}+u\frac{\partial v}{\partial x}+v\frac{\partial v}{\partial y}=-\frac{\partial p}{\partial y}+\frac{1}{\mathrm{Re}}\left(\frac{\partial^2 v}{\partial x^2}+\frac{\partial^2 v}{\partial y^2}\right)+\frac{1}{\mathrm{Fr}^2}+f_y, \tag{11}$$

It should be noted that, if the y dimension is considerably smaller than x dimension, and if the pressure difference between the inlet and the outlet flows, ΔP, is constant, the above Navier–Stokes equations reduces to

$$u=6\bar{u}\left(\frac{y}{w}-\frac{y^2}{w^2}\right), \tag{12}$$

Equation (12) is the parabolic velocity profile that has been used for field-flow fractionation FFF and most SPLITT calculations (1,2,20,21).

The DEM naturally assumes the presence of particles with a finite volume. To help couple the DEM particles to a viscous fluid flow, the concept of void fraction has been introduced into the DEM calculations to take into account the volume of the individual particles. The void fraction, ε, is defined as the ratio of fluid volume unoccupied by particles, V_{particle}, to the total fluid cell volume, V_{cell}:

$$\varepsilon=\frac{V_{cell}-\sum V_{particle}}{V_{cell}}. \tag{13}$$

Using the void fraction, the Navier-Stokes equation can be rewritten to calculate the average flow around the particles (37). The void fraction concept has been widely used in many solid–fluid systems such as fluidized bed processes (37,41,42).

Numerical Modelling of Particle Motion

The DEM traces particles in a system using the Newton's second law of motion.

$$\sum \mathbf{F}=m\mathbf{a} \tag{14}$$

Particle rotational motion is not included in this study.

As particles travel along the channel they may collide with each other or with the vessel walls. In the DEM, particle collisions may be modelled

by various ways, most commonly by the soft sphere and hard sphere models. In the soft sphere model, a spring, dashpot, and friction slider are used to describe particle interaction, which is assumed Voigt viscoelastic (37,41–43). Particles can also be treated as hard spheres as is commonly encountered in molecular dynamics simulation (44). In the hard sphere collision model, the particle velocity after the collision is calculated from the conservation of momentum equation. A restitution coefficient may be used to take into account of energy dissipation during the impact (38,43,45). For Brownian particles, various interparticle forces such as Van der Waals attraction, electrical double-layer repulsion, and short-range adhesive contact can be used (39). The lubrication effect of the viscous fluid layer between two particles may also be considered as an adjustment to the restitution coefficient or the spring constant (46,47).

Particle–Fluid Interactions

It is believed that there are a number of fluid forces present in the solid–fluid system that influence both particle and fluid behaviour (17,23,33). However, for simplification, in this study only the buoyancy and the drag forces were considered.

With the buoyancy effect included, the net force resulting in particle settling is defined as

$$F_s = \frac{4}{3}\pi r^3(\rho_p - \rho_f)g, \tag{15}$$

For the drag force, given the small particle size and the low Reynolds number of the fluid flow in a SPLITT channel, the simple Stokes drag equation was used

$$\mathbf{F}_d = -6\pi r\eta(\mathrm{U}_p - \mathrm{U}_f). \tag{16}$$

Aspects on 2D modelling of a 3D solid–fluid system have been well discussed in the literature (48). In this paper, particle and fluid behavior were studied at the central plane of the channel breadth, where negligible wall affects can be safely assumed.

RESULTS AND DISCUSSIONS

Comparison of SPLITT Theory, Simulation, and Experimental Data

In order to compare simulation results with SPLITT theoretical prediction, we disabled the particle–particle interaction and the effect of particle

momentum on fluid behavior. It should be noted that, such a setup allows the simulation to perform in a similar way to the approach of Zhang et al. (23,33) but in this case only the buoyancy and drag force were included in the algorithm.

Figure 2 shows the SPLITT channel model (not to scale) used in the simulations. Typical channel dimensions were chosen as follows: the channel length L was 10 cm. In order to simplify the grid structure, the total channel width w was set equal to 390 μm, and the splitters had a thickness of 130 μm and were placed as shown in Fig. 2. A channel breadth of 2 cm was used for some calculations to convert flow rates to axial velocities. The computational domain and fluid cells (not to scale) are indicated in the figure.

A small number of particles were evenly placed at the inlet and their exits at the two outlets were recorded. This particular initial boundary condition was used to compare the results of the simulation with SPLITT theory. Experimental run conditions from Springston et al. (10) were used for the simulation. Specifically, $\dot{V}(a') = \dot{V}(b) = 0.28\,\text{mL/min}$, and $\dot{V}(b') = \dot{V}(a)$ varied from 0.227 mL/min to 0.607 mL/min, and the particle diameter was 10 μm. While the channel thickness reported in the above paper was slightly different to that used in our calculations, 380 μm compared to 390 μm, the difference between the theory lines obtained from this study and from the experimental data was negligible (see Fig. 3).

Experimental data were scanned from the figures in the paper by Springston et al. and re-plotted together with the theoretically predicted trends and the simulation results. The very good match between the SPLITT theory and the simulation results verified the computer program for the DEM simulation. Following are two illustrative examples on

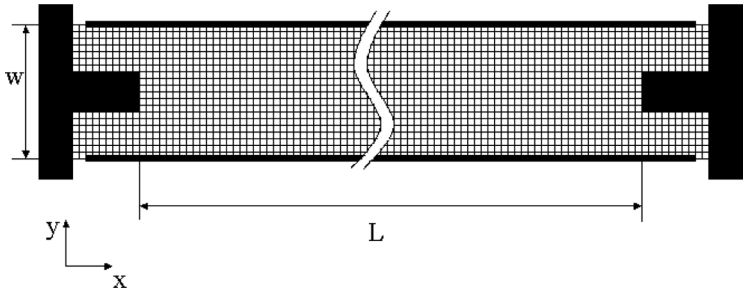

Figure 2. Simulation model for the SPLITT channel used in this study, which shows simulation domain and fluid grids (not to scale).

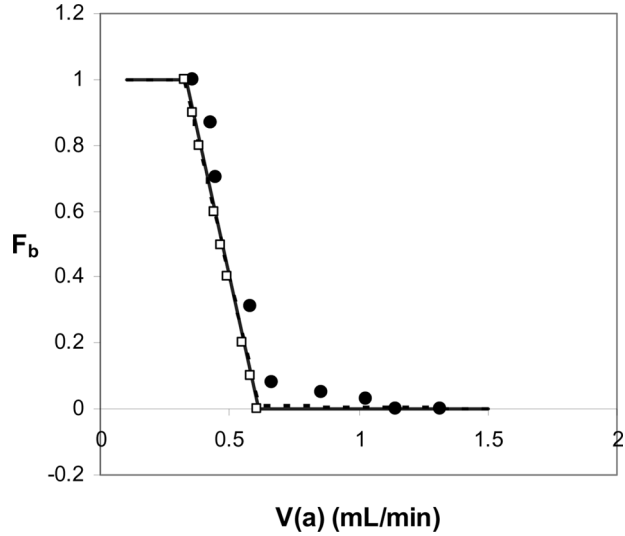

Figure 3. Comparison of SPLITT theory (solid line), simulation (hollow squares) and experimental results (filled circles) for the retrieval factor, F_b, for 10 μm particle. The dotted line is the SPLITT theoretical line calculated in Springston et al.(10) from which experimental data was also obtained.

1. the extent of possible particle collision and
2. the effect of particle motion on its surrounding fluid and, therefore, on the particle trajectory.

Estimation of the Extent of Particle Collision in a SPLITT Process

At very low Reynolds numbers, because lubrication forces between particles play an important role, theoretically, particles do not touch in this regime. For the purpose of the discussion on particle interactions, we will use the words ''collision'' to refer the process where the trajectories of two approaching particles change directions as a result of the interaction.

In the classical SPLITT theory, particles are treated as mass points and particle collisions are considered to have a negligible effect. In practice, to minimize particle interaction, very dilute sample solutions are used. A typical concentration of 0.1% (v/v) has been commonly considered as satisfactory for this assumption. However, the microdimensions of SPLITT channels make this assumption difficult to verify by microscopic observation. Some SPLITT researchers believe that particle

trajectories are affected to some extent by the shear-induced diffusion phenomenon, especially for concentrated suspensions often used in SPLITT fractionation. Shear-induced diffusion occurs when two particles, located in neighboring streamlines, change their distance from the channel wall. The overall tendency is for the faster moving particle (located at a larger distance from wall) passing the slower moving particle. It is believed these collision-like motions could be the reason behind the cross contamination effect, an undesired phenomenon that causes smaller particles entering the larger particle fraction stream and vice versa (49,50).

As DEM simulation can monitor individual particle motion, it provides an excellent tool to estimate the extent of particle collision under a particular SPLITT run condition. Depending on the particle interaction model used, the particle trajectory after a collision may vary. This, in turn, will determine the particle's subsequent collisions. However, if only the first collision of each particle is taken into account then the minimum number of collisions should be the same regardless of what collision mechanism is employed or whether a collision mechanism is included in the calculations. With that in mind, this study adopted the simplified case where a physical collision model was not employed and the effect of particle motion on the fluid flow was disabled. To find out whether particles collide when they travel down stream, we monitored individual particle movement using the Newton's second law of motion. A collision was detected when two particles crossed paths–approaching, overlapping, and then continuing on their paths. For an individual particle, only its first collision was taken into account. Subsequent collisions involving this particle were ignored. Results so obtained, effectively provided the theoretical minimum number of collisions associated with a particular run condition.

For this case study, the inlet flow rate $\dot{V}(a')(=\dot{V}(b))$ was first set to 0.28 mL/min, while the outlet flow rate $\dot{V}(a)(=\dot{V}(b'))$ varied in correspondence with $F_b = 0.1$, 0.4, 0.6 and 0.9. Five sample concentrations, 0.025, 0.05, 0.10, 0.15, and 0.20% (v/v), were used. The channel flow rate was then kept constant while both the inlet and outlet flow rates were allowed to vary to achieve the four values for F_b for sample concentration 0.10% (v/v). Monodisperse particle size distributions were used for each run. Particle sizes were 7, 10, and 15 μm. A total of 6000 particles for each size were randomly placed across the channel inlet (a') at fixed time steps according to the corresponding sample concentration

Collision results are tabulated in Tables 1 and 2. In Table 1 it was found that, even at extremely dilute concentrations (0.025% (v/v)), a small number of collisions were still detected. For all the three different particle sizes, more collisions were obtained for $F_b = 0.1$ and 0.9 than

Table 1. Number of particles (%) involving collision with other particles for 7, 10 and 15 μm particles in 5 different sample concentrations and 4 channel flow rates, together with their according retrieval factors. In all cases, inlet flow rates were 0.28 mL/min.

Conc. (%v/v)	$F_b = 0.1$	$F_b = 0.4$	$F_b = 0.6$	$F_b = 0.9$
7 μm				
	$\dot{V} = 0.69$ mL/min	$\dot{V} = 0.61$ mL/min	$\dot{V} = 0.55$ mL/min	$\dot{V} = 0.47$ mL/min
0.025	12.5	11.5	10.1	11.3
0.05	20.7	17.4	17.1	21.0
0.10	31.8	28.0	29.6	33.5
0.15	39.6	35.6	37.6	42.9
0.20	45.5	42.5	44.2	49.0
10 μm				
	$\dot{V} = 0.86$ mL/min	$\dot{V} = 0.77$ mL/min	$\dot{V} = 0.72$ mL/min	$\dot{V} = 0.63$ mL/min
0.025	5.5	4.9	4.3	4.7
0.05	14.0	12.5	11.8	12.4
0.10	26.2	23.0	22.6	25.4
0.15	35.4	32.0	31.0	35.2
0.20	41.3	38.0	37.6	41.6
15 μm				
	$\dot{V} = 1.26$ mL/min	$\dot{V} = 1.18$ mL/min	$\dot{V} = 1.12$ mL/min	$\dot{V} = 1.04$ mL/min
0.025	1.2	0.9	0.8	0.5
0.05	6.8	6.0	5.6	4.8
0.10	17.6	16.4	15.1	15.5
0.15	26.9	24.7	22.6	24.1
0.20	34.2	31.2	29.8	32.2

for $F_b = 0.4$ or 0.6 (Tables 1 and 2). This observation is consistent with theoretical prediction, as at $F_b = 0.1$ and 0.9, particles tend to travel in the regions closer to the upper and lower channel walls, where the fluid flow has higher shear. Also shown in the two tables, at the same F_b value, more collisions were counted for greater channel flow rates (higher shear).

For the same sample concentration, more collisions were detected for smaller particles. This is consistent with the theory as more (smaller) particles are required to make up the solution volume, hence there is a greater chance of collision. Whether this tendency is true in practice remains to be verified by experiment.

The initial entry conditions for the particles may also affect subsequent particle collisions. In this study, particles were randomly placed

Table 2. Number of particles (%) involving collision with other particles for 7, 10 and 15 μm particles at sample concentrations 0.1% (v/v), and at 4 different retrieval factors 0.1, 0.4, 0.6 and 0.9. For each particle size, channel flow rate was kept constant, while both inlet and outlet flow rates were varied and included in the Table. All flow rates are in mL/min.

Particle size (μm)	$F_b = 0.1$	$F_b = 0.4$	$F_b = 0.6$	$F_b = 0.9$
7	31.0%	29.8%	30.1%	33.5%
($\dot{V} = 0.47$ mL/min)	($\dot{V}_{(a')} = 0.16$, $\dot{V}_{(a)} = 0.31$)	($\dot{V}_{(a')} = 0.19$, $\dot{V}_{(a)} = 0.28$)	($\dot{V}_{(a')} = 0.22$, $\dot{V}_{(a)} = 0.25$)	($\dot{V}_{(a')} = 0.28$, $\dot{V}_{(a)} = 0.19$)
10	24.2%	22.3%	21.4%	25.4%
($\dot{V} = 0.63$ mL/min)	($\dot{V}_{(a')} = 0.16$, $\dot{V}_{(a)} = 0.47$)	($\dot{V}_{(a')} = 0.19$, $\dot{V}_{(a)} = 0.44$)	($\dot{V}_{(a')} = 0.22$, $\dot{V}_{(a)} = 0.41$)	($\dot{V}_{(a')} = 0.28$, $\dot{V}_{(a)} = 0.35$)
15	15.4%	15.1%	14.8%	15.5%
($\dot{V} = 1.04$ mL/ min)	($\dot{V}_{(a')} = 0.16$, $\dot{V}_{(a)} = 0.88$)	($\dot{V}_{(a')} = 0.19$, $\dot{V}_{(a)} = 0.85$)	($\dot{V}_{(a')} = 0.22$, $\dot{V}_{(a)} = 0.82$)	($\dot{V}_{(a')} = 0.28$, $\dot{V}_{(a)} = 0.76$)

across the channel inlet (a'). While it is a small effect, the number of collisions varies slightly for different random seeds. In reality, it is more likely that most particles enter the channel near the surface of the inlet splitter. This modelling approach could be effectively used to identify the right entrance conditions in order to reduce particle collisions.

Effect of Particle–Fluid Interaction on Particle Trajectory

By assuming that the fluid affects particle motion, but the particles do not affect the fluid, the local force system involving the particle and its surrounding fluid is not balanced. Most SPLITT studies assume that the particle size is small and typical SPLITT runs use an extremely dilute sample concentration, so the effect of the particle motion on the carrier fluid can be ignored (23). This assumption, however, has not been investigated to determine when it becomes invalid. To find out how particles will behave when the force system is more balanced, the effect of particle momentum upon the fluid behavior should be considered. Although, there is a wide range of particle–fluid interaction forces, in this study only the drag and buoyancy forces were included into the Navier Stokes equations, together with the void fraction calculations. This approach adapts the momentum exchange model developed and discussed in detail in Schwarzer et al. (48).

The same channel described in Section 4.2 was used to simulate particle trajectories for 7, 10, and 15 μm particles, with and without the effect of particle momentum on fluid velocities. We will use the terms

"uncorrected" and "corrected" to refer the case where the particle momentum effect on fluid velocities is disabled and enabled, respectively. Simulation results show this effect increases as the particle size increases, which is to be expected since both drag and buoyancy forces are size dependent. Figure 4 shows uncorrected and corrected trajectories for 15 μm particles; results for 7 and 10 μm are not included as the difference between corrected and uncorrected values are not significant.

A further simulation was conducted to investigate how this deviation affects the overall retrieval factor for each particle size. In order to isolate this effect from other factors (e.g. collisions) a simulation was run under extremely dilute particle concentration. A random number generator, was used to place 200 particles at the inlet entrance, 50% weighted toward the lower region of the inlet. The weighted random number was used to ensure uncorrected retrieval factor values, F_b, lying on the theory line. Particle trajectories were then monitored and their outlet exit was used for the calculation of their retrieval rate.

It was found that the difference between the corrected and the uncorrected values for F_b is unnoticeable for both 7 μm and 10 μm particles. A slight difference can be observed for 15 μm particles as shown in Fig. 5. However, when compared with experimental data, the contribution of this particular effect to the overall deviation from the theory line is still quite small for this size. The deviation from the theoretical line can be explained when a particle travels with a transverse velocity U slightly above its U_c, the uncorrected theory may include that particle into a smaller size sub-stream, while, in fact, it would exit the channel

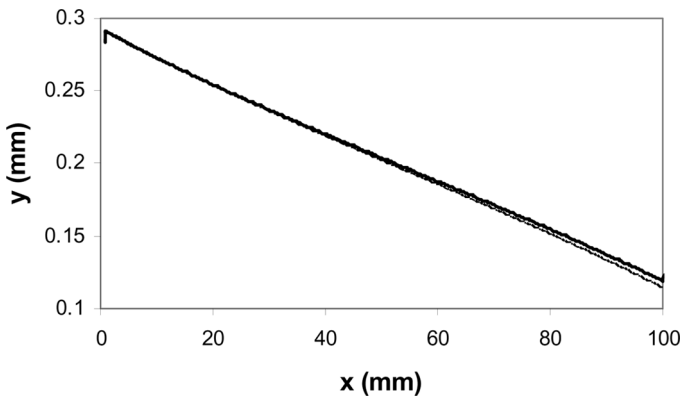

Figure 4. Comparison of particle trajectories obtained from standard theory (thick solid lines) and from simulation for 15 μm particle, where the latter includes the effect of particle motion on its surrounding fluid (thin lines).

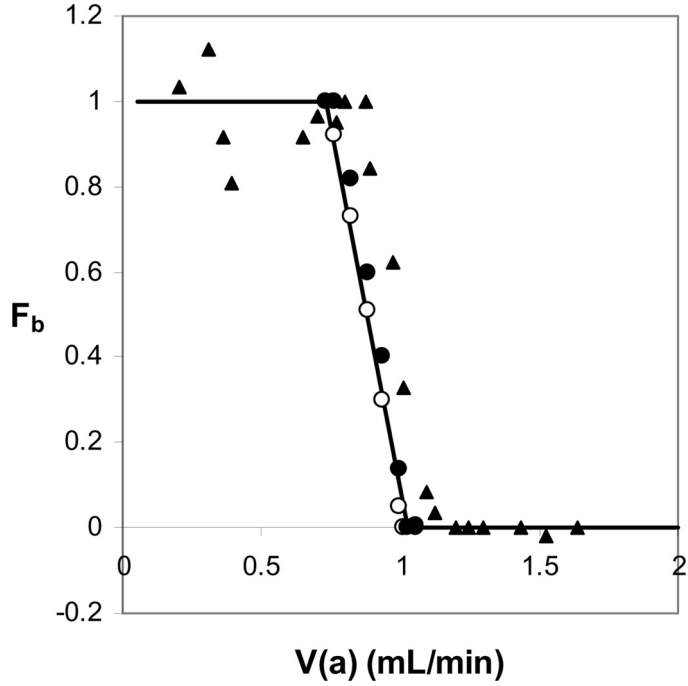

Figure 5. Illustration of the deviation of simulation results from the SPLITT theory line when the effect of particle motion on fluid behaviour was included in calculations for 15 μm particles. The solid line is from the theoretical prediction, hollow circles are for uncorrected simulation results, filled circles for corrected simulation results, and filled triangles are experimental data obtained from the Springston et al.(10).

via a larger size sub-stream. As a result, the measured retrieval rate for this particle size will be slightly higher than that predicted by the theory. However, since only a small particle population may fall within that velocity range, the overall effect is small.

This effect was also investigated for 10 μm particles at 3 different inlet flow rates, using the conditions described by Springston et al., in particular, $\dot{V}(a') = 0.05, 0.10,$ and 0.20 mL/min. Although the experimental results from Springton et al., show that F_b values tend to deviate more from the theoretical line when the channel flow rates increase, simulation results for this particle size show that, when the inlet flow rate increases the "particle on fluid" effect does not contribute to the overall deviation from the theory line. This indicates some other effects play a more important role in SPLITT separation, e.g. particle interactions

brought about by the increase in the inlet flow rate, which would increase the total shear in the channel flow (Figs. 6(a), (b), and (c)).

Simulation for the "particle on fluid" effect for larger particles was also attempted. We felt that it was more realistic to have the particles enter the channel from the lower region of the inlet, since it is more likely these particles would have settled somewhat nearer to the splitter surface. This entry can be achieved by using a random number generator 50% weighted toward the lower half of the channel inlet. When large particles (15 μm and greater) were forced to enter the channel in this way, their retrieval factors increased notably in comparison with the case where particles are evenly spread across the sample inlet stream (Fig. 7).

Simulations using 30 μm particles reveal the limit of particle size that can be used with the DEM simulation. For the numerical calculations to be meaningful, the fluid cell has to be large relative to the particle size.

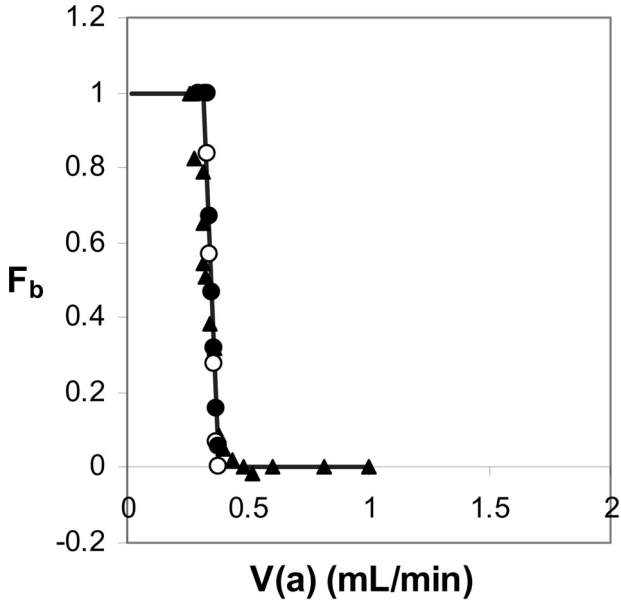

(a)

Figure 6. Illustration of the effect of particle-fluid interaction on particle retrieval factor F_b for 10 μm particles at 3 different inlet flow rates, which shows the effect is negligible for that particle size regardless of inlet/channel flow rates. In these figures, the solid line is from the theoretical prediction, hollow circles are for uncorrected simulation results, filled circles for corrected simulation results, and filled triangles are experimental data obtained from the Springston et al.(10).

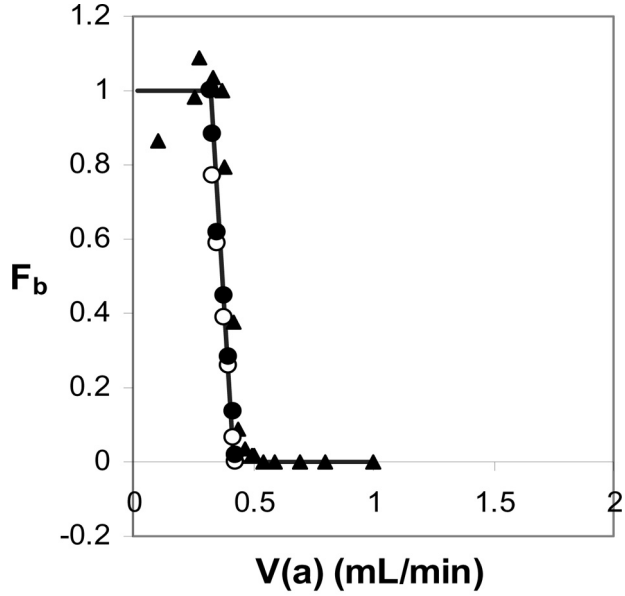

(b)

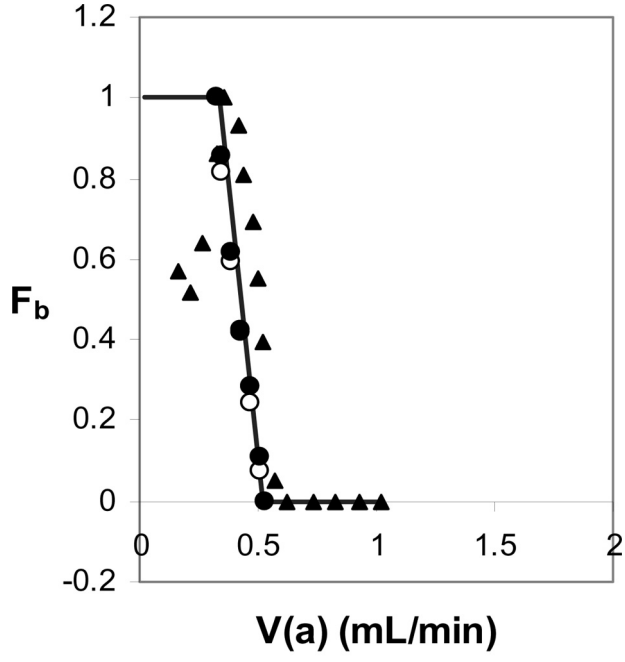

(c)

Figure 6. (Continued).

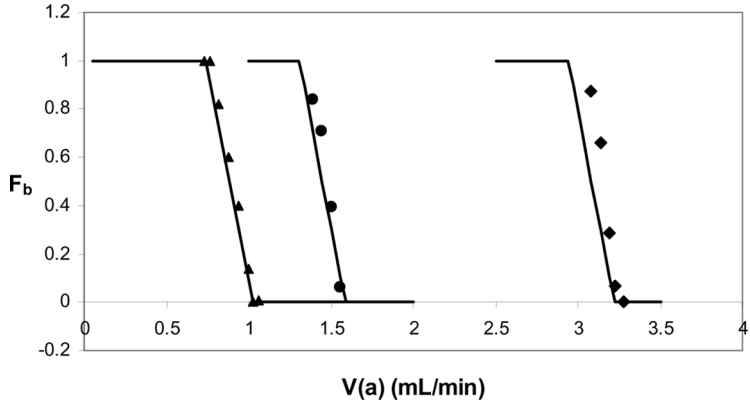

Figure 7. Illustration of the effect of particle-fluid interaction on particle retrieval factor F_b for particle size 15 μm (left), 20 μm (middle), and 30 μm (right), which shows the effect increases with particle size. Particle entry condition is 50% weighted toward ½ lower inlet region.

However, increasing the fluid cell size may sacrifice the accuracy of the fluid calculation, given the micro thickness of the SPLITT channel. More accurate calculations for both particle and fluid motion can be achieved by means of more expensive computational approaches such as the direct simulation method, which is outside the scope of this paper.

The above finding also indicates more work is needed to determine the conditions where a big particle, say 20 or 30 μm in size, can still be safely treated as a mass point in such a thin channel of 300–400 μm thickness. The outcome of such work would help to improve the SPLITT fractionation method for large particles.

While this paper shows that, for larger particles, particle motion may have some effect on its surrounding fluid, we are not yet able to compile generic guidelines for this effect.

CONCLUSIONS

This paper examines the usefulness of the discrete element method for SPLITT study. Our work starts with the simplest case in which, particle-particle collisions together with the effect of particle momentum on surrounding fluid were switched off. In such condition, the DEM results well agree with both SPLITT theory and experimental observations.

When particle discrete volume is considered, particle collisions can be detected. The possibility of particle collision is high even at very dilute sample concentration. For instance, if we consider 10 μm particles,

at typical concentration of 0.1%(v/v), then around 25% of particles are involved in collisions with other particles. This observation indicates the role of the interparticle and/or the lubrication forces may be significant in the SPLITT separation process.

For the effect of particle momentum on the surrounding fluid, the simulation found that in dilute sample concentration, the "particle on fluid" effect was either negligible or small for particle sizes up to 15 μm. More meaningful results could be obtained when an interparticle force is incorporated which allows all forces in the system to be considered. Nonetheless, simulation results show the DEM can be used for particle size up to 30 μm for this micro-dimensional system.

If an interparticle force is included, it would not only improve the accuracy for the SPLITT results, but also allow the technique to handle higher sample concentration. While it may be a challenging task to incorporate those forces into SPLITT theory analytically, the DEM provides SPLITT researchers with a much simpler way for testing their force hypotheses.

ACKNOWLEDGEMENT

This study was partially supported by the Victorian Partnership for Advanced Computing (VPAC), e-Research-8 Grant Scheme. The source code was provided by Vietec Pty. Ltd. The authors are grateful to Dr Anh Bui, CSIRO/MIT (Highett, Vic, 3190, Australia) for his help with some of CFD work.

NOMENCLATURE

$\dot{V}$	volumetric flow rate
U	particle field-induced velocity
b	channel breadth
L	channel length
d	particle diameter
$\Delta\rho$	difference between particle density and fluid density
ρ_f, ρ_p	fluid density and particle density, respectively
η	fluid absolute viscosity
g	the gravitational acceleration
x, y	axes of Cartesian system
u, v	fluid velocity components along x and y axes, respectively
t	time
p	fluid pressure
w	channel width

$\mathrm{Re} = \frac{lU_\infty}{\nu}$	Reynolds number, where l is the channel width, $l = w$
$\mathrm{Fr} = \sqrt{\frac{U_\infty}{gl}}$	Froude number, where l is the channel width, $l = w$
U_∞	fluid inlet velocity
$\bar{u}$	average fluid velocity
r	particle radius
$\mathrm{U_f}$, $\mathrm{U_p}$	fluid and particle velocity, respectively, in vector notation

REFERENCES

1. Giddings, J.C. (1968) Nonequilibrium theory of Field-flow fractionation. *J. Chem. Phys.*, *49* (1): 81–85.
2. Caldwell, K.D. (1988) Field-flow fractionation. *Anal. Chem.*, *60*(17): 959–971.
3. Myers M.N. (1997) Overview of field-flow fractionation. *J. Microcolumn Sep*, *9*: 151–162.
4. Giddings, J.C. (1985) A system based on Split-flow lateral-transport thin (SPLITT) separation cells for rapid and continuous particle fractionation. *Sep. Sci. Technol.*, *20*: 749–768.
5. Contado C; Dondi F; Beckett R; Giddings J.C. (1997) Separation of particulate environmental samples by SPLITT fractionation using different operating modes. *Analytica Chimica Acta*, *345*: 99–110.
6. Blo G; Conato C; Contado C; Fagioli F; Dondi F. (2004) Quantitative SPLITT fractionation of lagoon sediments. *Annali di Chimica*, *94*: 617–627.
7. Fuh, C.B.; Giddings, J.C. (1995) Isolation of human blood cells, platelets, and plasma proteins by centrifugal SPLITT fractions. *Biotechnol. Prog.*, *11*: 14–20.
8. Fuh C.B; Giddings J.C. (1997) Separation of submicron pharmaceutic emulsions with centrifugal Split-flow thin (SPLITT) fractionation. *J. Microcolumn Sep.*, *9*: 205–211.
9. Benincasa, M.A.; Moore, L.R.; Williams, P.S.; Poptic E.; Carpino, F.; and Zborowski, M. (2005) Cell sorting by one gravity SPLITT fractionation. *Anal. Chem.*, *77*: 5294–5301.
10. Springston, S.R.; Myers, M.N.; Giddings, J.C. (1987) Continuous particle fractionation based on gravitational sedimentation in Split-flow thin cells. *Anal. Chem.*, *59*: 344–350.
11. Gao Y.; Myers M.N; Barman B.N; Giddings J.C. (1991) Continuous fractionation of glass microspheres by gravitational sedimentation in Split-flow thin (SPLITT) cells. *Part. Sci. Technol.*, *9*: 105–118.
12. Fuh, C.B.; Myers, M.N.; Giddings, J.C. (1994) Centrifugal SPLITT fractionation: New technique for separation of colloidal particles. *Ind. Eng. Chem. Res.*, *33*: 355–362.
13. Giddings, J.C. (1989) Harnessing electrical forces for separation: capillary zone electrophoresis, isoelectric focusing, Field-flow fractionation, Split-flow Thin-cell continuous-separation and other techniques. *J. Chromatogr. A*, *480*: 21–33.

14. Giddings, J.C. (1988) Continuous separation in split-flow thin (SPLITT) cells: potential applications to biological materials. *Sep. Sci. Technol.*, *23*: 931–943.
15. Levin, S.; Myers, M.N.; Giddings, J.C. (1989) Continuous separation of proteins in electrical Split-flow thin (SPLITT) cell with equilibrium operation. *Sep. Sci. Technol.*, *24*: 1245–1259.
16. Zborowski, M; Williams, P.S.; Sun, L; Moore, L.R. (1997) Chalmers, J.J., Cylindrical SPLITT and quadrupole magnetic field in application to Continuous-flow magnetic cell sorting. *J. Liq. Chromatogr. Relat. Technol.*, *20* (16 & 17):2887–2905.
17. Zhang, Y.; Emerson. D.R.; and Reese, J.M. (2003) General theory for flow optimization of Split-flow thin fractionation. *J. Chromatogr. A*, *1010*: 87–94.
18. Mandralis, Z.I.; Feke, D.L. (1993) Continuous suspension fractionation using acoustic and Divided-flow fields. *Chem. Eng. Sci.*, *48* (23): 3897–3905.
19. Beckett, R; TRi, N; Tangtreamjitmun, N and Morrison, R., Use of Acoustic SPLITT Fractionation to Measure the Mechanical Properties of Particles, L-26, The Tenth International Symposium on Field-flow Fractionation, Amsterdam, the Netherlands 2002.
20. Williams, P.S; Levin S.; Lenczycki, T; and Giddings, J.C. (1992) Continuous SPLITT fractionation based on a diffusion mechanism. *Ind. Eng. Chem. Res.*, *31*: 2172–2181.
21. Williams, P.S. (1994) Particle trajectories in field-flow fractionation and SPLITT fractionation channels. *Sep. Sci. Technol.*, *29* (1): 11–15.
22. Liang-Shih Fan and Chao Zhu (1998) *Principle of Gas Solid Flow*, Arvind Varma, Eds. Cambridge University Press, U.K.
23. Zhang, Y.; Barber, R.W.; and Emerson, D.R. (2005) Particle separation in microfluidic Devices–SPLITT fractionation and microfluidics. *Curr. Anal. Chem.*, *1* (3): 345–354.
24. Gupta, S; Ligrani, P.M; Myers, M.N; Giddings J.C. (1997) Resolution deterioration and optimal operating conditions in centrifugal SPLITT fractionation. Part I: Stable density gradients. *J. Microcolumn Sep.*, *9* (3): 213–223.
25. Gupta, S; Ligrani, P.M; Myers, M.N; Giddings J.C. (1997) Resolution deterioration and optimal operating conditions in centrifugal SPLITT fractionation. Part I: Unstable density gradients. *J. Microcolumn. Sep.*, *9* (4): 307–319.
26. Gupta, S; Ligrani, P.M and Giddings, J.C. (1997) Investigations of performance characteristics including limitations due to flow instabilities in continuous SPLITT fractionation. *Sep. Sci. Technol.*, *32*: 1629–1655.
27. Caughey, D.A and Hafez, M.M. (2000) *Frontiers of Computational Fluid Dynamics-2000*, Caughey, D.A and Hafez, M.M., Eds. World Scientific Publishing, Singapore.
28. Caughey, D.A and Hafez, M.M. (2002) *Frontiers of Computational Fluid Dynamics 2002*, Caughey, D.A and Hafez, M.M., Eds. World Scientific Publishing, River Edge, New Jersey.
29. Fuh, C.B.; Trujillo, E.M.; Giddings, J.C. (1995) Hydrodynamic characterization of SPLITT fractionation cells. *Sep. Sci. Technol.*, *30* (20): 3861–3876.

30. Williams, P.S; Decker, K; Nakamura, M; Chalmers, J.J; Moore, L.R; Zborowski, M. (2003) Splitter imperfections in annular Split-flow thin separation channels: experimental study of nonspecific crossover. *Anal. Chem., 75*: 6687–6695.
31. Williams, P.S; Moore, L.R; Chalmers, J.J; and Zborowski, M. (2003) Splitter imperfections in annular Split-flow thin separation channels: effect on nonspecific crossover. *Anal. Chem.*, *75*: 1365–1373.
32. Nguyen, M; Liffman, K; Rudman, M; McKinnon, I., and Beckett, R, Computational Modelling and Simulation of Fluid Flows and Particle Transport in a SPLITT Fractionation Channel, A-24, the 10th International Symposium on Field-Flow Fractionation, Amsterdam, The Netherlands, 2002.
33. Zhang Y; Emerson D.R. (2004) Effect of flow development region and fringing magnetic force field on annular split-flow thin fractionation. *J. Chromatogr. A*, *1042*: 137–145.
34. Cundall, P.A.; Strack, O.D.L. (1979) A discrete numerical model for granular assemblies. *Geotechnique*, *29*: 47–65.
35. Leary, P. (2001) Modelling comminution devices using DEM. *Int. J. Numer. Anal. Meth. Geomech.*, *25*: 83–105.
36. Mishra, B.K; Rajamani, R.J. (1992) The discrete element method for the simulation of ball mills. *Appl. Math. Modelling*, *16*: 598–604.
37. Tsuji, Y; Kawaguchi, T.; and Tanaka, T. (1993) Discrete particle simulation of two-dimensional fluidized bed. *Powder Technology*, *77*: 79–87.
38. Liffman K.; Nguyen M.; Metcalfe G.; Cleary P. (2001) Forces in piles of granular material: an analytic and 3D DEM study. *Granular Matter*, *3*: 165–176.
39. Li, J-F; Yu, W-H; Chen, C-S; and Wei, W-C J. (2003) Modeling Nanosized Colloidal Particle Interactions with Brownian Dynamics Using Discrete Element Method, Chapter 12: Computational Methods and Numerics, Nanotech 2003 Vol. 2, Technical Proceedings of the 2003 Nanotechnology Conference and Trade Show, California, USA.
40. Fletcher, CAJ. (1991) *Computational Techniques for Fluid Dynamics*, Vol. II, 2nd Ed, Springer-Verlag, New York.
41. Mikami, T.; Kamiya, H.; Horio, M. (1998) Numerical simulation of cohesive powder behavior in a fluidized bed. *Chem. Eng. Sci.*, *53*: 1927–1940.
42. Rhodes, M.J; Wang, X.S; Nguyen, M; Stewart, P; Liffman, K. (2001) Study of mixing in Gas-fluidized beds using a DEM model. *Chem. Eng. Sci.*, *56*: 2859–2866.
43. Liffman, K, Chan, D. Y. C. and Hughes, B. D. (1992) Force distribution in a two dimensional sandpile. *Powder Technology*, *72*: 255–267.
44. Allen, M. P; and Tildesley, D. J. (1990) *Computer Simulations of Liquids*, Oxford Science Publications, Oxford.
45. Hoomans, B.P.B.; Kuipers, J.A.M.; Briels, W.J; and Swaaij, W.P.M. (1996) Discrete particle simulation of bubble and slug formation in a Two-dimensional Gas-fluidised bed: A hard-sphere approach. *Chem. Eng. Sci*, *51*: 99–118.
46. Davis, RH; Serayssol J-M; Hinch E.J. (1986) The elastohydrodynamic collision of two spheres. *J. Fluid Mech.*, *163*: 479–497.

47. Zhang, W.B; Noda, R; Horio, M. (2005) Evaluation of lubrication force on colliding particles for DEM simulation of fluidized beds. *Powder Technology*, *158* (1–3): 92–101.
48. Schwarzer, S. (1995) Sedimentation and flow through porous media: Simulating dynamically coupled discrete and continuum phases. *Phys. Review E. part B*, *52* (6): 6461–6475.
49. Michel Martin, Ecole Supérieure de Physique et de Chimie Industrielles, Laboratoire de Physique et Mécanique des Milieux Hétérogènes, UMR CNRS 7636, 10, rue Vauquelin, 75231 Paris Cedex 05, France, personal communication
50. Contado, C.; Hoyos, M. (2007) SPLITT cell analytical separation of silica particles. Non-specific crossover effects: does the shear-induced diffusion play a role?, *Chromatographia*, *65* (7-8): 453–462.